Electronic Supplementary Material (ESI) for Dalton Transactions.

Supporting Information

Topochemical Reaction Induced the formation of Bi_2S_3 Micro-straws from Bi-MOF for Ultra-long Zn Storage Life

Lei Gou,*[a] Kai Liang,[a] Wen-Yan Wang,[a] Ya-Ting Lei,[a] Shou-Lin Xie,[a] Ding-Kai Wei,[a] Dong-Lin Li[a] and Xiao-Yong Fan*[a]

[a] Institute of Energy Materials and Electronic Device, School of Materials Science and Engineering, Chang'an University, Xi'an 710061, China

*Corresponding authors: leigou@chd.edu.cn (L Gou); xyfan@chd.edu.cn (X.Y. Fan)

Synthesis of the Bi_2S_3-TF

Bi_2S_3-TF was also chemically synthesized by a solvothermal method. $Bi(NO_3)_3 \cdot 5H_2O$ (50 mg) and thiourea (CH_4N_2S, 100 mg) were mixed in a mass ratio of 1:2 and added into a 20 mL absolute ethanol solution, which was sonicated for 30 min, and then stirred for 30 min. The mixture was transferred into a PTFE-lined stainless steel autoclave and kept at 160 ℃ for 6 h before cooling down to room temperature. The resulting product was dried in air overnight after filtering, washed thoroughly with ethanol and water, and labeled as Bi_2S_3-TF.

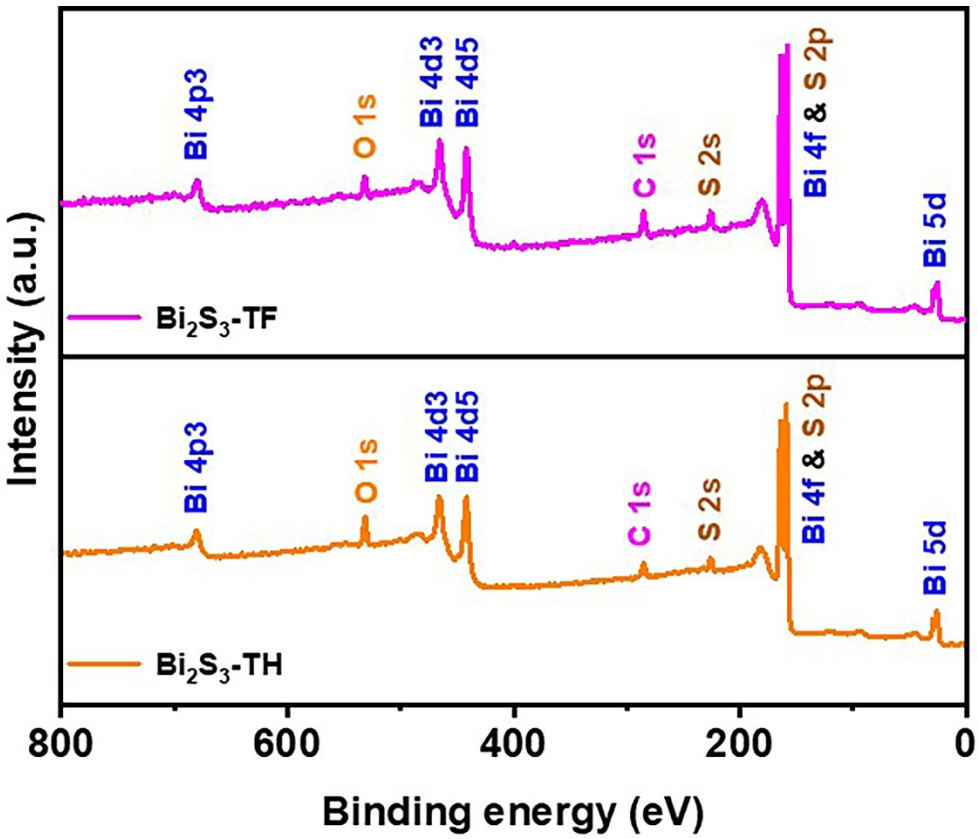

Figure S1. High-resolution XPS fine spectra of Bi_2S_3-TH and Bi_2S_3-TF

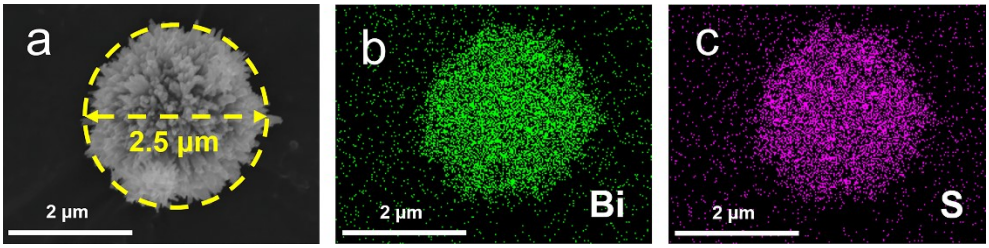

Figure S2. SEM images of the Bi_2S_3-TF products and corresponding EDS analysis of Bi and S their elemental mapping (b and c).

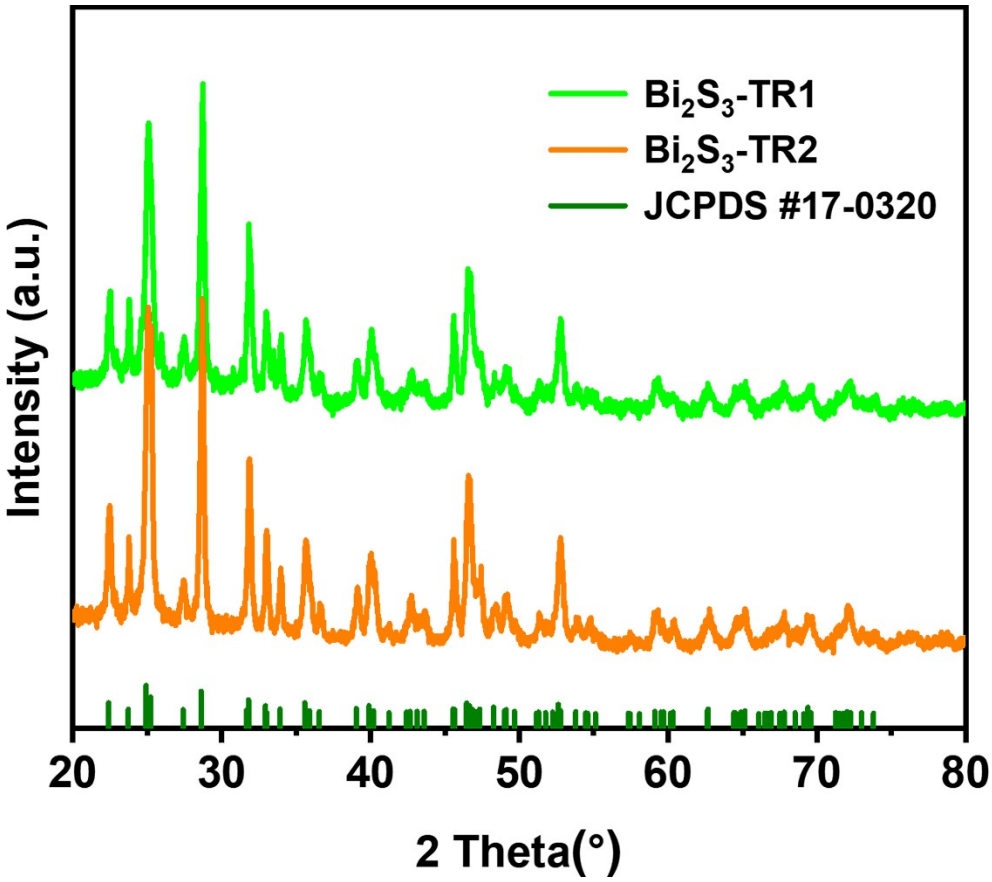

Figure S3. XRD patterns of the Bi_2S_3-TR1 and Bi_2S_3-TR2

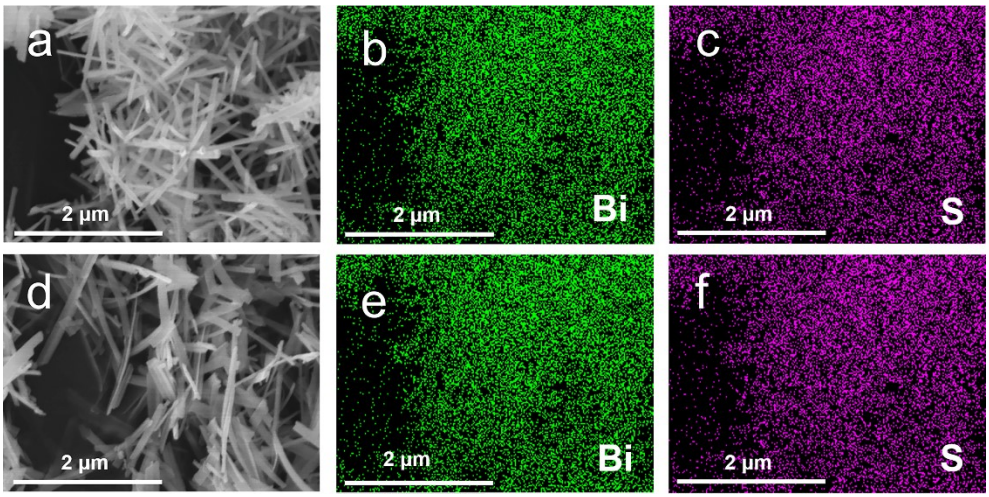

Figure S4. (a) SEM images of the Bi_2S_3-TR1 products and corresponding EDS analysis of Bi and S their elemental mapping (b and c), (d) SEM images of the Bi_2S_3-TR2 products and corresponding EDS analysis of Bi and S their elemental mapping (e and f).

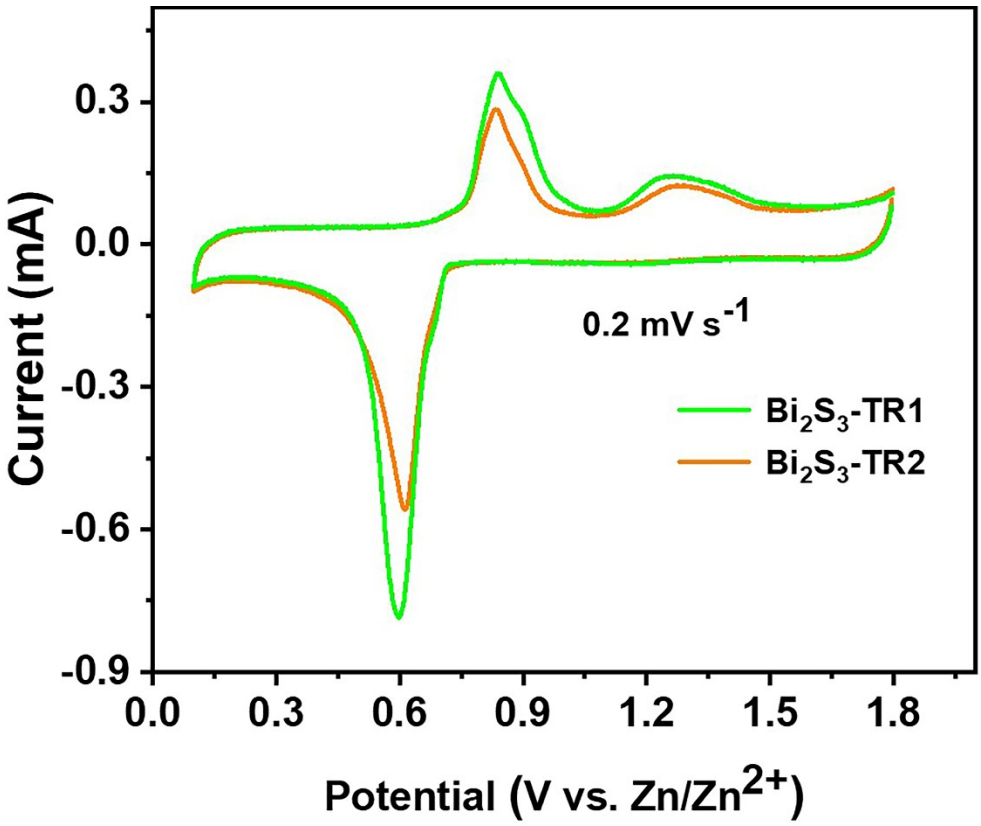

Figure S5. CV profiles of the Bi_2S_3-TR1 and Bi_2S_3-TR2 electrodes at 0.2 mVs^{-1} in an aqueous electrolyte of 3M $ZnSO_4$.

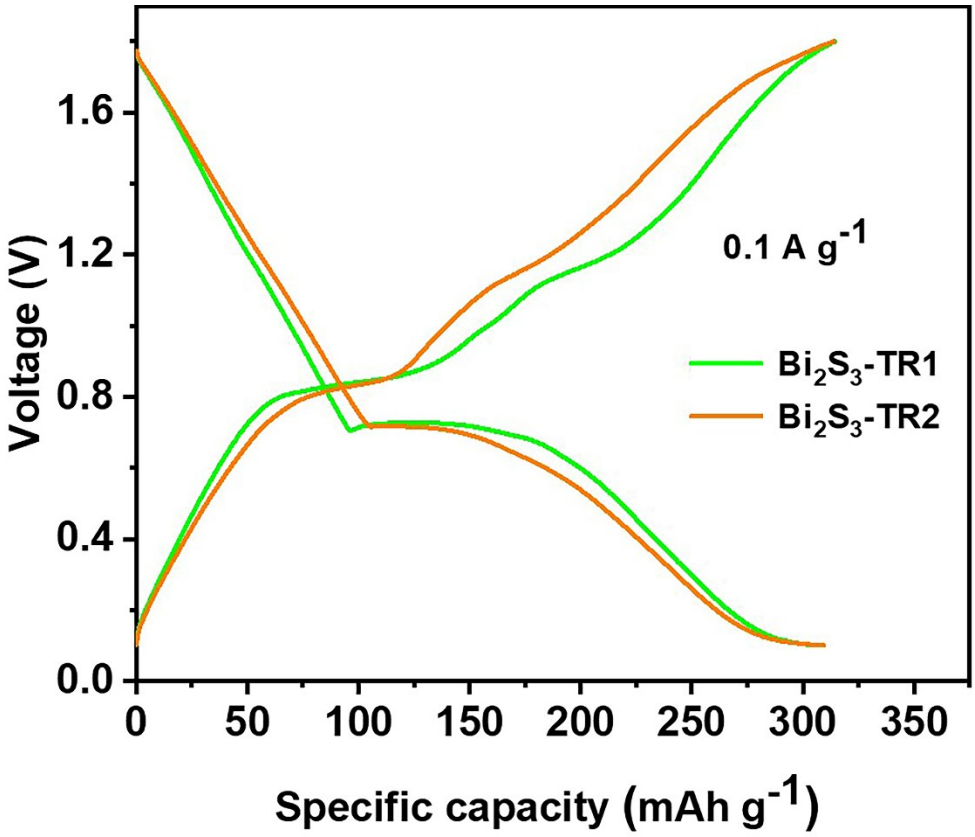

Figure S6. Discharge-charge profile of the Bi_2S_3-TR1 and Bi_2S_3-TR2 electrodes at a current density of 0.1 A g^{-1}.

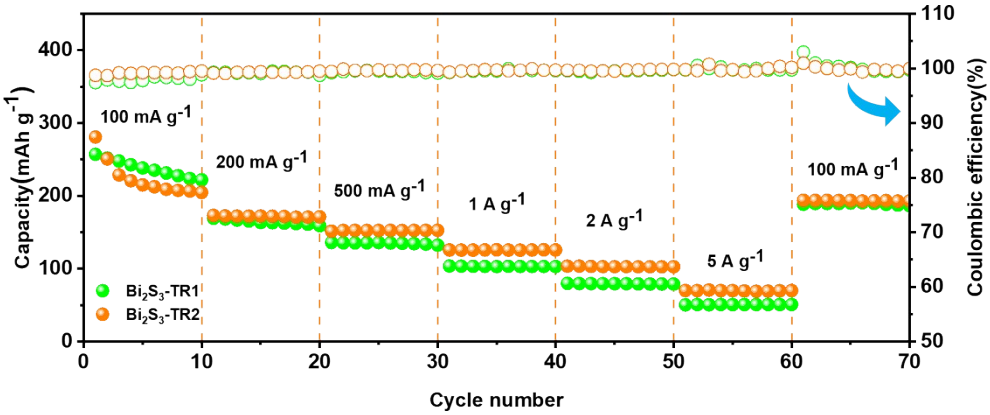

Figure S7. Rate capability at 0.1-5 A g^{-1} of Bi_2S_3-TR1 and Bi_2S_3-TR2

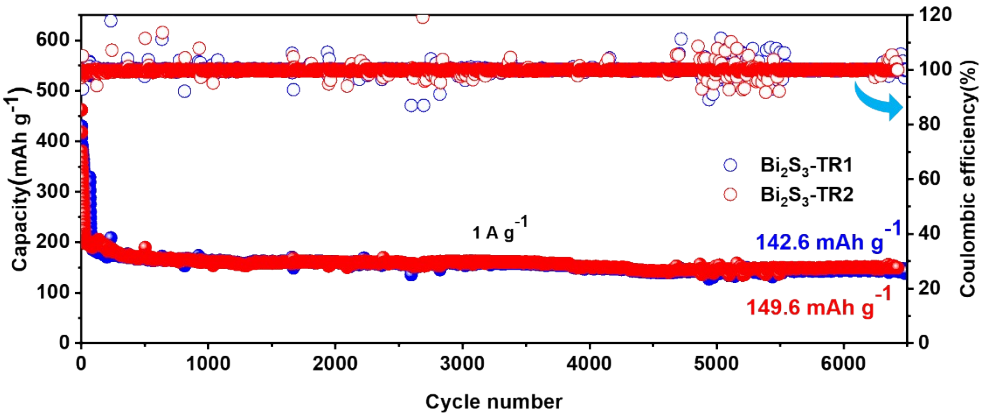

Figure S8. Long-term cycling stability at 1 A g^{-1} of Bi_2S_3-TR1 and Bi_2S_3-TR2.

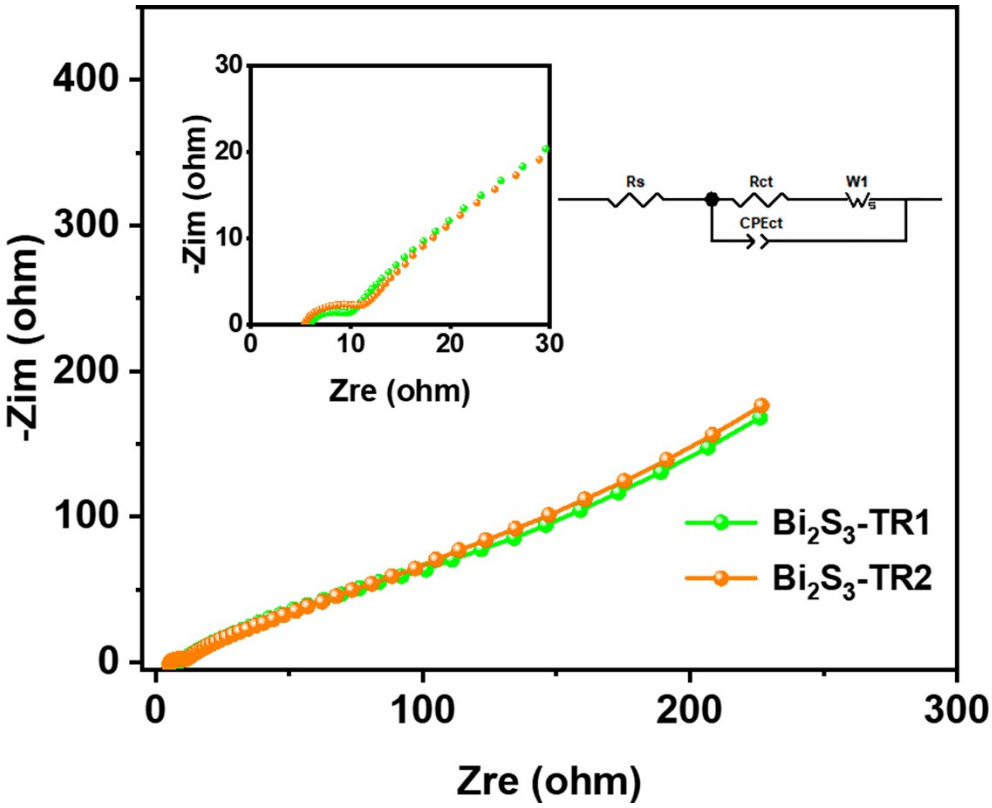

Figure S9. Nyquist plots of Bi_2S_3-TR1 and Bi_2S_3-TR2 electrode.

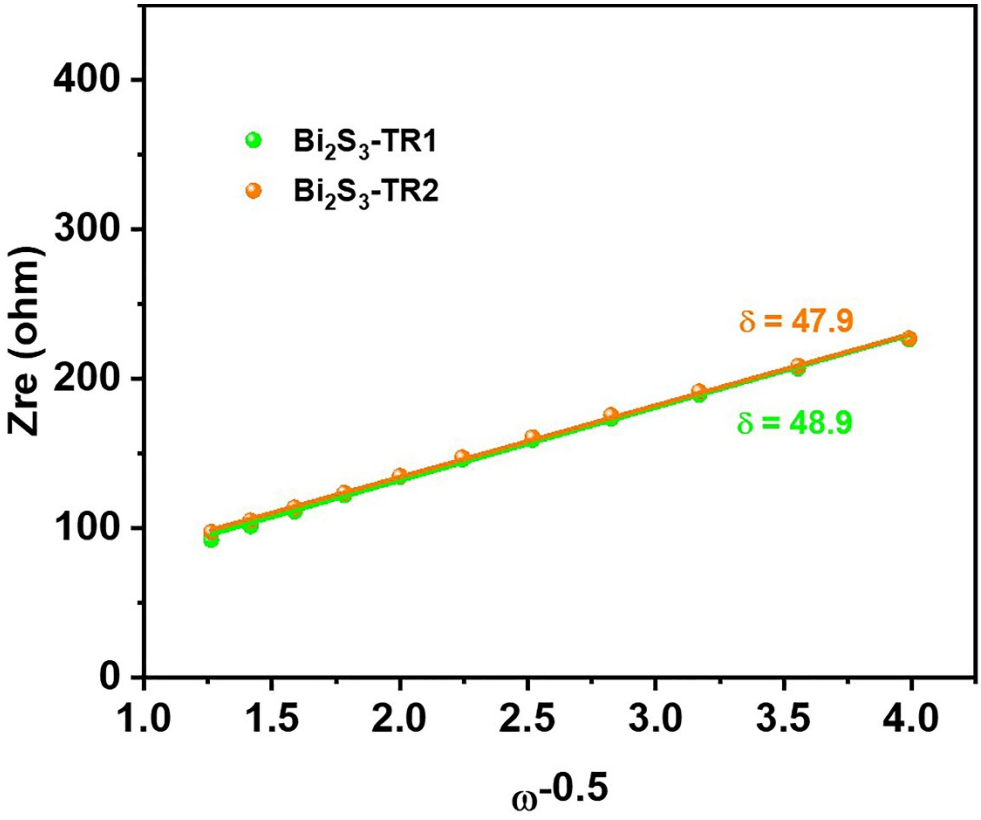

Figure S10. The plots of real parts of the complex impedance versus $\omega^{-0.5}$.

Table S1. EIS data statistics of Bi_2S_3 electrode

Sample	R_s (Ω)	R_{ct} (Ω)	σ	D
Bi_2S_3-TH	3.45	5.47	26.5	1.13168E-10
Bi_2S_3-TF	2.58	16.79	82.6	1.16481E-11
Bi_2S_3-TR1	5.66	5.98	48.9	3.32351E-11
Bi_2S_3-TR2	5.07	7.08	47.9	3.46373E-11